Bioresource Technology 293 (2019) 122101

Contents lists available at ScienceDirect

Bioresource Technology

journal homepage: www.elsevier.com/locate/biortech

Carbon sequestration pathway of inorganic carbon in partial nitrification sludge

Xiaoning Liu[a], Huaqin Wang[a], Haixiang Li[a], Yue Jin[b], Wenjie Zhang[a,*]

[a] Guangxi Key Laboratory of Environmental Pollution Control Theory and Technology, College of Environmental Science and Engineering, Guilin University of Technology, Guilin 541004, PR China

[b] College of Civil Engineering and Architecture, Guilin University of Technology, Guilin 541004, PR China

GRAPHICAL ABSTRACT

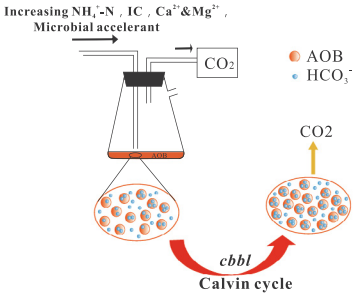

ARTICLE INFO

Keywords:
Ammonia-oxidizing bacteria
Inorganic carbon
^{13}C isotopic abundance
Gene abundance

ABSTRACT

Inorganic carbon is an important carbon source of autotrophic bacteria, e.g., ammonia-oxidizing bacteria. Ammonia-oxidizing bacteria are chemoautotrophic bacteria with carbon sequestration capacity. Experiments were performed on partial nitrification sludge with different influent matrices, and optimal experimental operational conditions were established. The carbon fixation pathway of ammonia-oxidizing sludge was determined via ^{13}C isotope tracers and qPCR. The denitrification effect was better when the NH_4^+-N, HCO_3^-, Ca^{2+}, Mg^{2+}, and microbial accelerant concentrations were 15, 250, 113, 100 and 1 mL/L, respectively. The nitrite accumulation rate reached 96.95%. ^{13}C isotope tracing showed that ^{13}C abundance in sludge increased significantly. The results showed that IC added into the influent participated in the carbon metabolism of microorganisms. The functional gene *cbbL*, which follows the Calvin cycle carbon sequestration pathway, was identified in the ammonia-oxidizing bacteria, and the effect of influent NH_4^+-N on the gene abundance was greater than that of other substrates.

1. Introduction

Anaerobic ammonia oxidation (anammox), a relatively new autotrophic denitrification method, has developed into an efficient, economical, and environmentally friendly alternative to traditional denitrification processes (Okabe et al., 2011). In this biological process, nitrite and ammonium are directly converted to nitrogen and water without oxygen and organic carbon. Anammox has the advantages of higher nitrogen removal rates, lower operation costs, lower surplus sludge yields, and lower space requirements (J Gijs, 2008; Ma et al., 2016; Meng et al., 2017). Full-scale anammox has been successfully applied to the treatment of high-nitrogen wastewater, including

* Corresponding author.
E-mail address: 2010053@glut.edu.cn (W. Zhang).

https://doi.org/10.1016/j.biortech.2019.122101
Received 15 July 2019; Received in revised form 29 August 2019; Accepted 31 August 2019
Available online 04 September 2019
0960-8524/

Table 1
Composition of wastewater used in the experiments.

Groups Components	A				B				C				D			
(mg/L)	A1	A2	A3	A4	B1	B2	B3	B4	C1	C2	C3	C4	D1	D2	D3	D4
$(NH_4)_2SO_4$	10	15	20	30	15				15				15			
$NaHCO_3$	250				150	250	500	750	250				250			
$CaCl_2{\cdot}2H_2O$	110				110				55	110	170	200	110			
$MgSO_4{\cdot}7H_2O$	100				100				50	100	150	175	100			
Microbial accelerant (mL/L)	1				1				1				0.5	1	1.5	1.75
$Na_2S_2O_3$	20				20				20				20			
KH_2PO_4	50				50				50				50			

digested sludge, landfill leachate, and pharmaceutical wastewater (Jin & Zhang, 2016; Lackner et al., 2014; Strous et al., 1998; Yamamoto et al., 2007).

Partial nitrification is a preprocess in anammox and uses ammonia-oxidizing bacteria (AOB) to oxidize a proportion (about 56%) of NH_4^+-N in wastewater to NO_2^--N under aerobic conditions (Wei et al., 2018). It is a necessary pretreatment, because anammox depends on the concentration ratio of NH_4^+-N to NO_2^--N in inflow water. Anammox bacteria convert NO_2^--N and residual NH_4^+-N to nitrogen under anaerobic conditions, thus shortening the redox process from NH_4^+-N to N_2 (Kartal et al., 2010). Therefore, partial nitrification is key to the successful operation of anammox to efficiently produce NO_2^--N from sludge. The key microorganisms in the combined process of anammox and partial nitrification are AOB and anammox bacteria, which are chemoautotrophic microorganisms (Strous et al., 1999a). They can use inorganic carbon (IC) as a carbon source for their own cell synthesis, so they have a certain carbon sequestration capacity (Wang et al., 2018), so that the process of anammox and partial nitrification does not need additional organic carbon sources (Jetten et al., 2002). In partial nitrification, IC is not only an important carbon source for bacterial assimilation but also plays an important role in the regulation of biochemical reactions, e.g., microbial activity (Guisasola et al., 2006). Therefore, AOB activity can be promoted by the addition of IC, and NO_2^--N can consequently be efficiently produced during partial nitrification.

Hitherto, five CO_2 fixation pathways have been identified, namely the pentose phosphate cycle (Calvin cycle), reductive acetyl coenzyme A pathway, 3-hydroxypropionate bicycle, reductive tricarboxylic acid cycle, and 3-hydroxypropionate/4-hydroxybutyrate and 4-hydroxybutyrate cycles (Benson & Calvin, 1950; Buchanan & Arnon, 1990; Ragsdale, 1991; Shively et al., 1998; Sylvia et al., 2002). The Calvin cycle is the main CO_2-fixation pathway in photoautotrophic microorganisms and chemoautotrophic bacteria (Ragsdale, 1991). Ribulose 1,5-diphosphate carboxylase/oxygenase is the key enzyme controlling the cycle rate. The properties of the enzyme are directly related to the fixation rate of atmospheric CO_2.

Rubisco and its coding gene *cbbL* have been extensively studied in laboratory environments. By using isotope tracing and determining enzymatic activity, Stefan (2004) inferred that different AOB could have the same carbon fixation pathway, possibly the Calvin cycle or acetyl coenzyme A pathway. Strous et al. (1999b), by using macro genomic technology, found that the genome of *Candidatus Kuenen stuttgartiensis* contained all the genes encoding the key enzymes of the acetyl coenzyme A pathway, showing that anaerobic AOB immobilized carbon through the acetyl coenzyme A pathway.

However, few studies have been done on the carbon sequestration potential of partial nitrification sludge in the anammox process, especially in terms of the mechanism. In this study, AOB in partial nitrification during anammox were simulated and sampled in real time from different substrates at various concentrations to establish the optimal reaction conditions. IC in influent water was labeled with ^{13}C isotope tracers, ^{13}C isotope abundance in sludge was detected via stable isotope mass spectrometry, and the AOB carbon fixation pathway was determined via microbial molecular qPCR technology.

2. Materials and methods

2.1. Inoculated sludge and test water

The influent water was artificially simulated wastewater. Matrix conditions with different substrates were divided into four groups: NH_4^+-N, IC, Ca^{2+} and Mg^{2+}, and microbial accelerant (Ruicheng Environmental Protection Consulting Company, Weifang, Shandong, China), named groups A to D, respectively. The microbial accelerant was based on enzymatic enhancers, which can enhance the activity of biological reactions and promote proliferation (Wang et al., 2019). These four groups were subdivided into four more groups (Table 1). The influent pH was adjusted by 0.5 mol/L NaOH and 0.5 mol/L H_2SO_4 buffer solutions (Zhang & Jin, 2017). The inoculated sludge in the experiment was a partial nitrification sludge domesticated and cultured in the laboratory (Jin et al., 2015). Partial nitrification performance was tested by using the nitrite accumulation rate (NAR). The closer the NAR is to 100%, the better the partial nitrification effect is (Dong et al., 2013). The NAR in this study was > 99%.

2.2. Experimental setup

This study used a sequencing batch reactor, and the material was plexiglass (Ma et al., 2019). Three groups of parallel reaction devices were used. The volume of the reactor was 0.5 L, the hydraulic retention time was 1.5 h, and the temperature, pH, and dissolved oxygen were maintained at 32 ± 1 °C, 7.5 – 7.8, and 0.5 mg/L, respectively, via water bath heating (Jin et al., 2015). Fig. 1 schematically illustrates the device and experimental setup.

The siphon method was used for the test water intake and outlet. To let water in, one end of the intake pipe (silica gel tube) was connected to the intake of the device and the other end to the artificial wastewater. When the water was discharged, the silica gel tube was placed in the supernatant, and the outlet was sealed during the operation of the reactor. When the influent water was replaced, all the previously treated water was removed and replaced with ready-made artificial wastewater.

2.3. Analytical methods

The effluent and influent of each reactor was stored in a 50 mL sampling bottle after passing through a 0.45 μm filter membrane. After sampling, the samples was detected immediately or placed in a refrigerator at 4 °C for testing (Wenjie et al., 2014). Partial nitrification sludge was stored in a refrigerator at −20 °C for molecular experiments. The water quality indexes were determined in this experiment using NH_4^+-N, NO_2^--N, total nitrogen, and IC. NO_2^--N and NH_4^+-N via the colorimetric method according to standard methods (Jin et al., 2016b), and total nitrogen via alkaline potassium persulfate ultraviolet

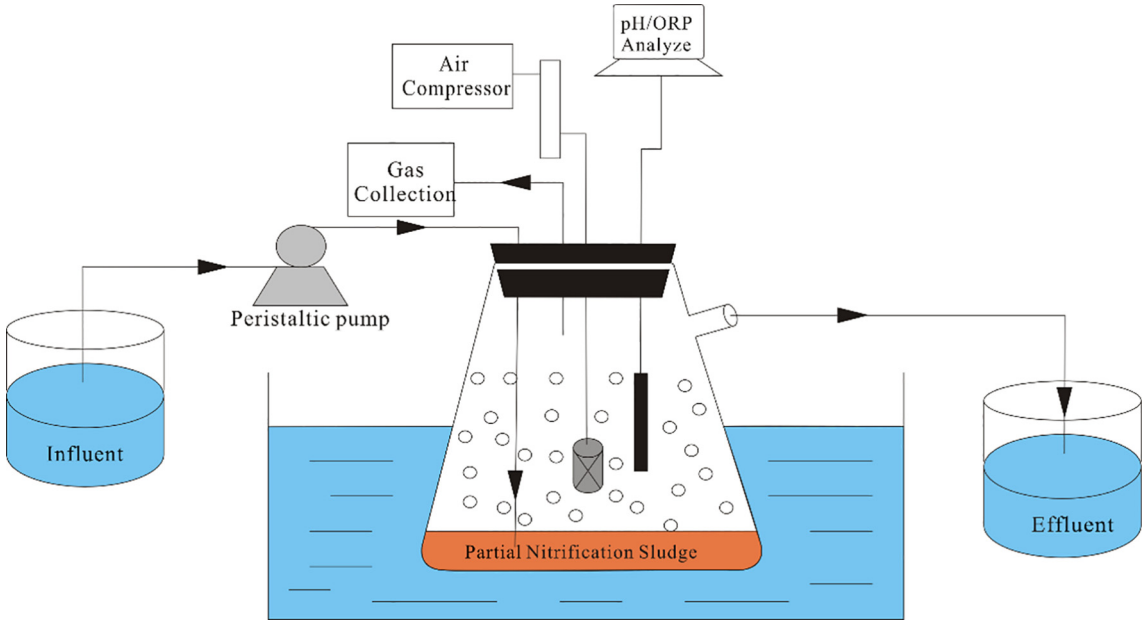

Fig. 1. Schematic diagram of partial nitrification reactor. Influent, influent tank; Effluent, effluent tank; Peristaltic pump, influent pump; Gas collection, gas collecting bag.

spectrophotometry (Zhang et al., 2015). IC was detected via the total organic carbon analysis method with a total organic carbon analyzer (Multi N/C 3100, Analytik Jena, Germany) (Zhang et al., 2018). The pH/temperature was determined by PHS-3C acidity meter (Lei Ci, Shanghai Instrument and Electrical Science Instruments Co., Ltd.,China) and DO was determined by portable dissolved oxygen meter HQ30d (Hach, USA).

2.4. Analysis of CO_2 gas

CO_2 gas was collected via a gas sampling bag at the exhaust valve at the top of the gas collection barrel (Jin et al., 2016a). The CO_2 content in gas samples was determined via gas chromatography (Shanghai Jingke GC-112A, China) developed by the N(VI)2000 Chromatography Data Workstation (Institute of Intelligent Information, Zhejiang University, China). The concentration of CO_2 standard gas (produced by Shanghai Shenkai Gas Co., Ltd., China) was 4.92%, and the equilibrium gas was argon. Chromatographic conditions were as follows: The carrier gas flow rate was 4.0 mL/min, injector temperature was 70 °C, column box temperature was 35 °C, detector temperature was 120 °C, detector current was 110 mA, and injection volume was 1 mL. The CO_2 content in the sample was calculated using equation (1). Each gas sample was measured at least three times to obtain an average value.

$$C_{CO2=}C_s \times A_{CO2}/A_s \quad (1)$$

where C_{CO2} is the CO_2 content of the gas sample (mL), A_{CO2} is the peak area of CO_2 in the gas sample ($\mu V{\cdot}s^{-1}$), C_s is the CO_2 content in standard gas (mL), and A_s is the peak area of CO_2 in standard gas ($\mu V{\cdot}s^{-1}$).

Carbon sequestration rate was calculated by Formula (2).

$$\text{Carbon sequestration rate} = \frac{IC_{inf.} - IC_{eff.} - 0.273 \times CO_2 \times \rho_{CO_2}}{IC_{inf.}} \quad (2)$$

where $IC_{inf.}$ is the input IC during 24 h, mg; IC_{eff} is the output IC during 24 h, mg; CO_2 is the CO_2 production during 24 h, mL; ρ_{CO2} is the density of CO_2, g/L; The CO_2 density is approximately 1.781 mg/mL under conditions of 30 °C and 101 kPa.

2.5. ^{13}C abundance detection

The ^{13}C isotope-labeled $NaHCO_3$ was used as the IC source in the intake water. The experimental devices were composed of BLK, E, F, and G groups. E, F, and G were three groups of parallel reaction devices using $NaHCO_3$ as the influent IC source, and BLK was a reaction device using ordinary $NaHCO_3$ as the influent IC source. The treated isotope sludge was analyzed via stable isotope mass spectrometry (Delta V Advantage, Thermo, German). The C isotope value of the sample was ^{13}C (VPDB). The ^{13}C abundances of the sample were calculated according to equation (3):

$$13C\ (\%) = 100 * (\delta 13C * R_r + 1000\ R_r) / (\delta 13C * R_r + 1000\ R_r + 1000) \quad (3)$$

where R_r represents $^{13}C/^{12}C = 0.0112372$ in the VPDB standard sample, and $\delta^{13}C$ is the measured carbon isotope value (VPDB).

2.6. DNA extraction and quantitative PCR

The initial sludge and groups A–D were frozen at −20 °C. Total DNA was extracted from the granular sludge using the Power Soil® DNA Isolation Kit (MoBio 12888–50, USA). The concentration and purity of extracted DNA were determined via micro-ultraviolet spectrophotometry (Q5000, Quawell, USA) (Wang et al., 2019; Zhang et al., 2016).

Quantitative PCR (qPCR) was performed using primer pairs *cbbL*R1-F/*cbbL*R1-R (forward primer was AAG GAY GAC GAG AAC ATC and reverse primer was TCG GTC GGS GTG TAG TTG AA) for the red-type Rubisco form I *cbbL* gene for the Calvin cycle (Selesi et al., 2005). The purified PCR products were ligated into T-vectors using the pEASY®-T3 Cloning Kit (TransGen Biotech, China) and then transformed into Trans 1-T2 Phage Resistant Chemically Competent Cells. Positive clones (white colonies) were randomly selected, and the plasmid DNA was extracted using the Plasmid DNA Mini-Preps Kit (Sangon Biotech, China). Ten-fold serial dilutions of the plasmid DNA with a known copy number were used to plot a standard curve.

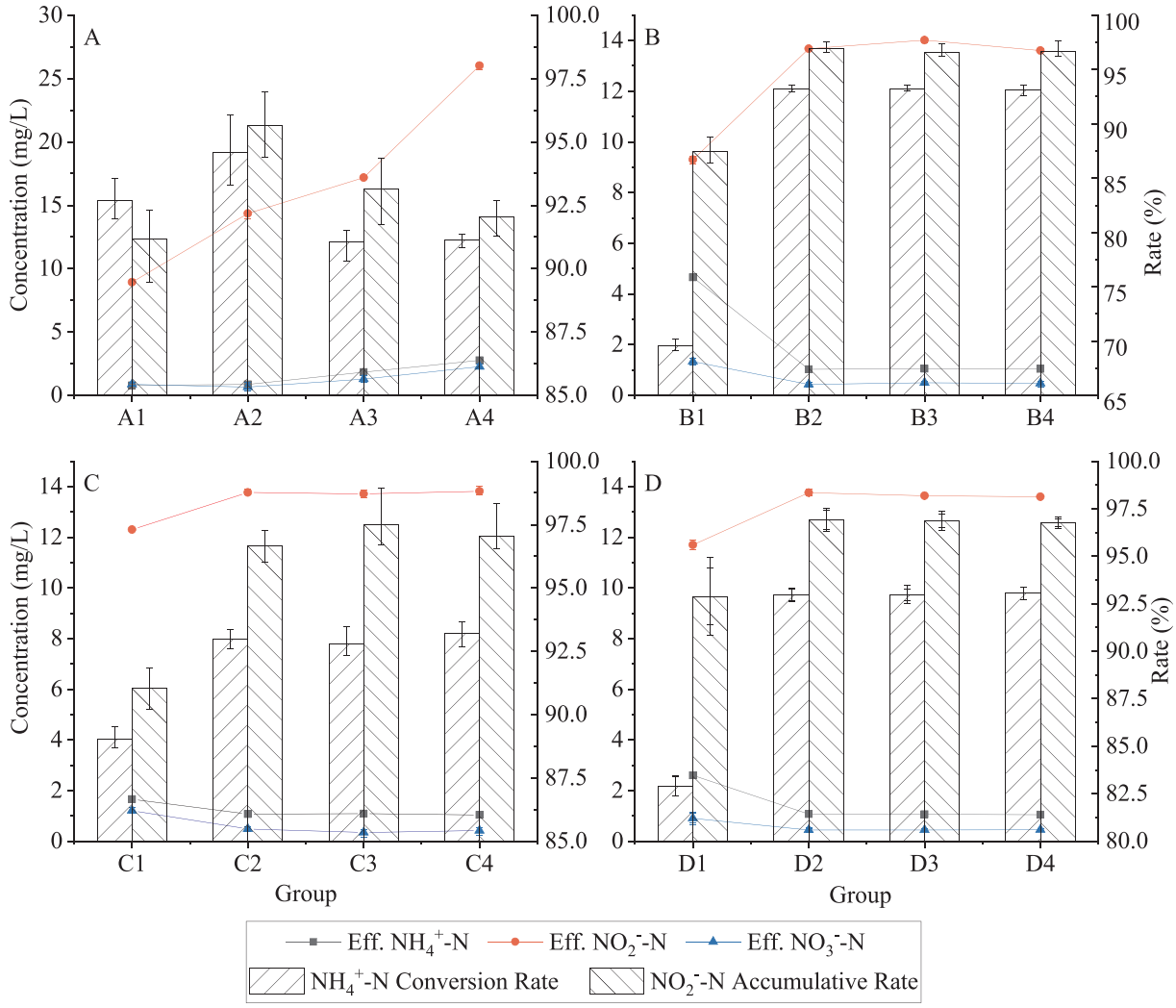

Fig. 2. Changes in nitrogen under different influent matrix conditions. A, effect of influent NH_4^+-N; B, effect of influent inorganic carbon (IC); C, effect of influent Ca^{2+} and Mg^{2+}; D, effect of microbial accelerant.

3. Results and discussion

3.1. Nitrogen removal performance

Fig. 2 shows the changes in nitrogen in the groups A–D. The inoculated sludge was obtained from the partial nitrification sludge domesticated and cultured in laboratory and had a NAR of 99.4%. Therefore, each group of sludge had a good NAR. Fig. 2A shows the nitrogen changes in groups A1, A2, A3, and A4 under different influent NH_4^+-N concentrations. With increased influent NH_4^+-N, the highest NH_4^+-N conversion and NO_2^--N accumulation rates (57 and 95.65%, respectively) occurred in A2. The effluent NH_4^+-N, NO_2^--N, and NO_3^--N concentrations were 0.86, 14.34, and was 0.65 mg/L, respectively. Increasing the NH_4^+-N concentration of influent may decrease the partial nitrification activity. The conversion rate of NH_4^+-N in A1 was higher than the accumulation rate of nitrous nitrogen, which may be due to the low concentration of influent NH_4^+-N, the conversion of some NH_4^+-N into NO_2^--N, and the volatilization and escape of some NH_4^+-N. The relatively high concentration of effluent NO_3^--N in A4 may be due to excessive aeration and dissolved oxygen. Therefore, the highest nitrogen accumulation rate of partial nitrification sludge was 95.65%, when the influent concentration of NH_4^+-N was 15 mg/L in group A.

IC is a substrate for autotrophic bacteria and has an important impact on their normal metabolism; it therefore also impacts AOB. Fig. 2B shows the changes in nitrogen in B1–B4 under different influent IC concentrations. In B1, the conversion rate of NH_4^+-N was 69.57%, and the effluent NH_4^+-N concentration was 4.65 mg/L. The low conversion rate under this condition may be due to the low concentration of HCO^{3-} in the influent. The conversion rates of NH_4^+-N in B2, B3, and B4 were similar at 93.26, 93.25, and 93.12%, respectively. The NAR in B2–B4 was 96.95, 96.60, and 96.69%, respectively. The NAR was therefore the lowest in B1, but the NO_3^--N concentration in B1 effluent was the highest. Based on the NH_4^+-N conversion rate, it is further speculated that the low IC concentration in the influent may be the result of the inhibition of partial nitrification. There was almost no change in the NAR value of the B2-B4 group. Therefore, when the influent IC concentration was 250 mg/L, sufficient carbon source could be supplied for the ammonia oxidizing bacteria to utilize itself, and the NAR is 96.95%.

Ca^{2+} and Mg^{2+} are indispensable elements for the growth of microorganisms and affect microorganism activity and immobilization (Macêdo et al., 2019). Fig. 2C shows the changes in nitrogen under different influent Ca^{2+} and Mg^{2+} concentrations. The Ca^{2+} and Mg^{2+} concentrations in C1 were too low, and the NH_4^+-N conversion rate was also relatively low at 89.04%. With increased Ca^{2+} and Mg^{2+} concentrations, the conversion rate of NH_4^+-N in C1 increased correspondingly, but that in C2–C4 were maintained at around 92.99, 92.78, and 93.19%, respectively. The NAR in C1–C4 was 91.03, 96.65, 97.51, and 97.03%, respectively. The highest accumulation rate occurred in C2 but did not differ much from that in C3 and C4. The results showed

that the concentration of Ca and Mg had little effect on partially nitrification when they reached 110 mg/L and 100 mg/L respectively. Therefore, these concentrations of Ca^{2+} and Mg^{2+} were suitable for the growth of partial nitrification sludge and the NAR was 96.65%.

Fig. 2D shows the changes in microbial accelerants. Therefore, the microbial accelerant concentration affected microbial activity. When the microbial accelerant concentration increased from 0.5 to 1 mL/L, the NH_4^+-N conversion rate increased from 82.91 to 92.97%. With increased microbial accelerant concentration, the NH_4^+-N conversion rate did not change significantly in the D3, D4 (92.98 and 93.05%, respectively). In the experiment, the accumulative rate of NO_2^--N was above 90%. Except for the slightly lower accumulative rate of NO_2^--N in group D1, the accumulative rate of the other three groups was almost the same. The NH_4^+-N conversion rate and NAR were relatively stable when the microbial accelerant concentration increased to 1 mL/L and the NAR was 96.92%. According to the NAR of each experimental group, the partial nitrification sludge had a good conversion rate, and only $NaHCO_3$ was added as IC source during the experiment. According to Wang et al. (2018), IC can be used as a carbon source for AOB cell synthesis, which has a certain carbon sequestration capacity. Therefore, this process did not require additional organic carbon sources to provide energy for AOB.

3.2. Effect of matrix amount on carbon sequestration

Fig. 3 shows the relationship between carbon sequestration and different influent matrix concentrations in groups A and B. Carbon sequestration was determined by subtracting the influent IC content from the effluent IC content and carbon content of the CO_2 emissions. As shown in Fig. 3A, the influent NH_4^+-N content increased from 10 to 30 mg/L, and the average carbon sequestration rate of IC increased accordingly from 3.42 to 7.91%. Therefore, the relationship between influent NH_4^+-N and carbon sequestration rate was fitted (Fig. 3a) and described by Eq. (3):

$$y = 0.000834x^2 + 0.19496x + 1 \quad R^2 = 0.98052 \tag{3}$$

where y is carbon sequestration, and $\times$ is the influent NH_4^+-N content. There was a positive correlation between the influent NH_4^+-N content and carbon fixation rate from equation (3): The carbon fixation rate increased with increasing influent NH_4^+-N. However, excessive influent NH_4^+-N led to the release of CO_2 into the system. Considering the NH_4^+-N conversion rate and NAR, the optimum influent NH_4^+-N concentration was 15 mg/L.

Fig. 3B shows the relationship between the carbon sequestration rate and IC content in group B. With increasing influent IC content, the average carbon sequestration rate decreased gradually from 6.59 to 1.75%. Therefore, the fitting of the relationship between influent IC

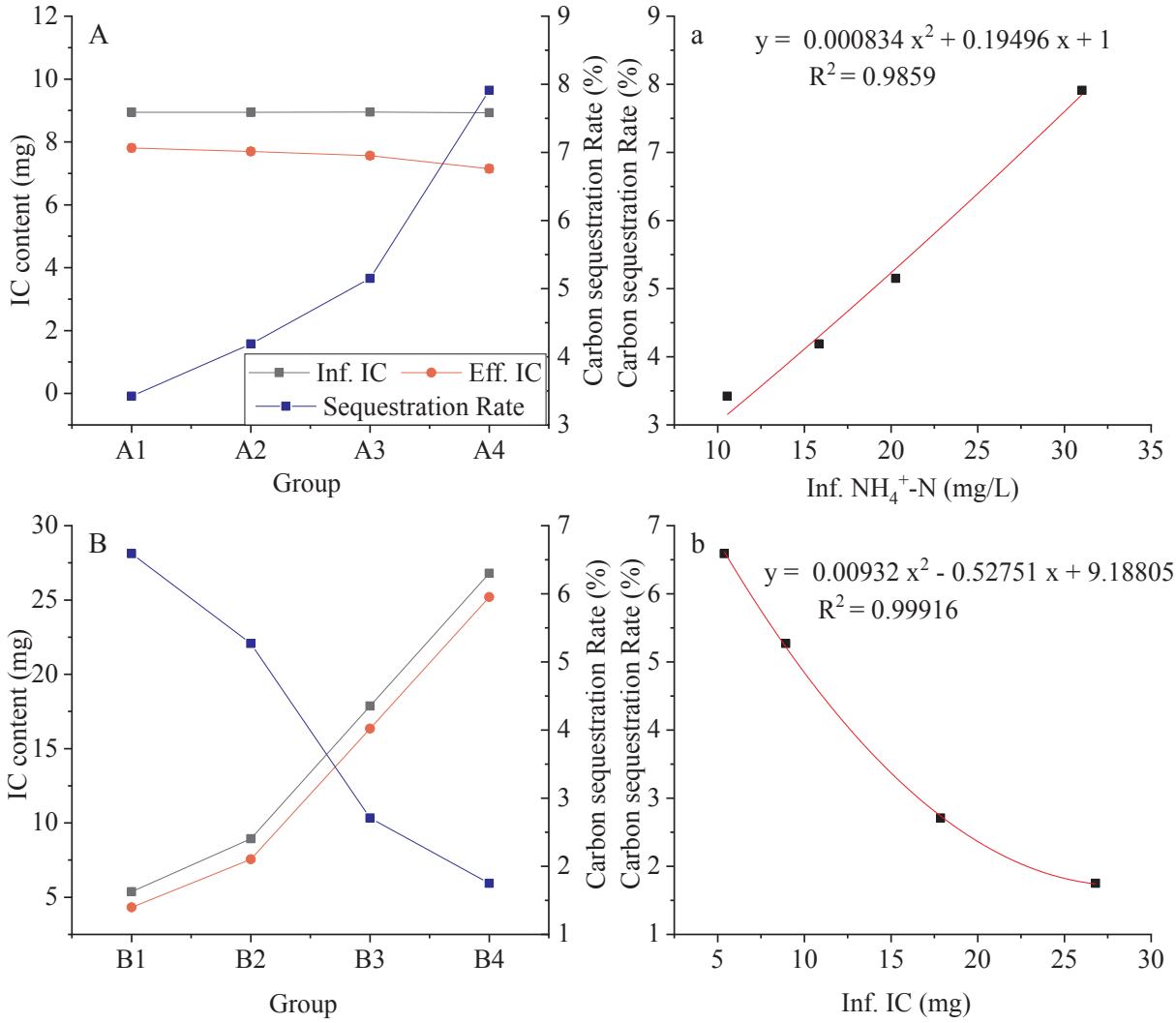

Fig. 3. Relationship between different influent matrix conditions and carbon sequestration. Figure left: A, effect of influent NH_4^+-N; B, effect of influent inorganic carbon (IC); Figure right: a, relationship between influent (Inf.) NH_4^+-N and carbon sequestration rate; b, relationship between IC and carbon sequestration rate.

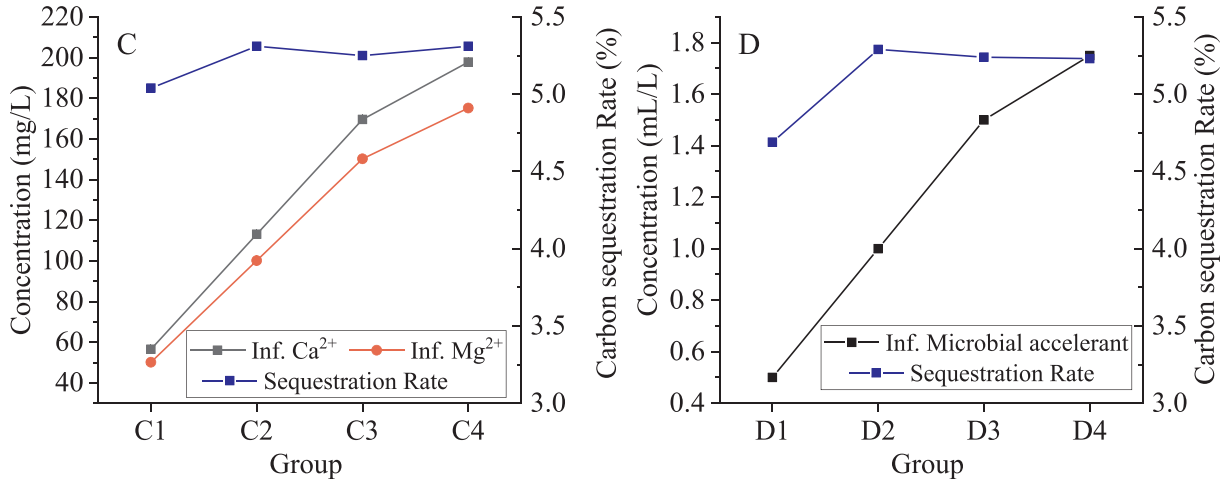

Fig. 4. Relationship between concentration of influent matrix and carbon sequestration. C, effect of influent Ca^{2+} and Mg^{2+}; D, effect of microbial accelerant.

Table 2
Experimental results of ^{13}C isotope experimental group.

Parameter Group	C%	$\delta^{13}C$	^{13}C%	NH_4^+-N conversion rate (%)	NO_2^--N accumulative rate (%)	Carbon sequestration rate (%)
Blank sample	39.01	−40.79	1.066	92.85	97.69	5.34
IEG*	33.35 ± 2.18	161.3 ± 16.33	1.29 ± 0.02	93.17 ± 0.45	97.13 ± 0.33	5.26 ± 0.04
P-value	0.153**	0.009	0.009	0.600**	0.282**	0.197**

Notes:
* IEG, isotope experimental group
** There was significant correlation at 0.05 level (bilateral).

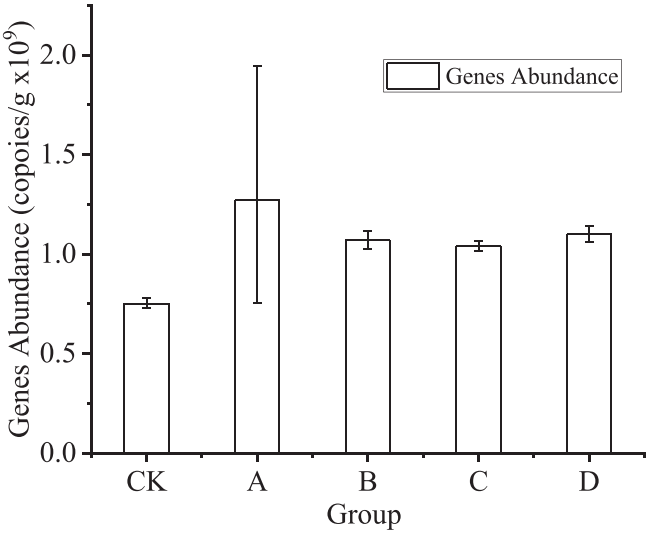

Fig. 5. Correlation between *cbbL*R1 gene abundance and matrix factor in partial nitrification sludge. Note: Error bars express standard deviation.

content and carbon sequestration rate in Fig. 3b was described by Eq. (4):

$$y = 0.00932x^2 - 0.52751x + 9.18805 \quad R^2 = 0.99916 \tag{4}$$

where y is carbon sequestration, and $\times$ is the influent IC content. The relationship between IC in influent water and average carbon sequestration rate was negatively correlated. The lower IC concentration can inhibit the partial nitrification. An increased IC concentration can improve the NH_4^+-N conversion rate and NAR, but too much IC may lead to increased release of CO_2 into the system. When enough IC is added, the carbon sequestration rate of the system is relatively stable. In this

Table 3
Correlation between *cbbL*R1 gene abundance and matrix factor in partial nitrification sludge.

Correlation	Nitrogen	IC	Ca^{2+} and Mg^{2+}	Microbial Accelerators
R^2	0.998	0.984	0.831	0.886
P-value	0.002**	0.016**	0.170*	0.114*

Notes:
* Significant correlation was found at 0.05 level (bilateral).
** There was significant correlation at 0.01 level (bilateral).

experiment, 250 mg/L HCO^{3-} met the normal operation of partial nitrification.

The relationship between Ca^{2+} and Mg^{2+} concentrations and average carbon sequestration rate is shown in Fig. 4C. The average carbon sequestration rate of C1 increased from 5.04 to 5.31%, whereas those of C2–C4 were relatively stable at 5.31, 5.25, and 5.31%, respectively. Although Ca^{2+} and Mg^{2+} are essential elements for microbial growth, they had no significant effect on the denitrification performance and carbon sequestration rate of the system. Therefore, to maintain normal operation of the system, the Ca^{2+} and Mg^{2+} concentrations should be 113.12 and 100.14 mg/L respectively.

The effect of microbial accelerants on the carbon sequestration rate is shown in Fig. 4D. When the microbial accelerant concentration increased from 0.5 to 1 mL/L, the average carbon sequestration rate of the system increased from 4.69 to 5.29%. However, with the continuous increase of microbial accelerant concentration, the average carbon sequestration rate remained relatively stable between 5.24 and 5.23%, respectively. The microbial accelerant concentration had little impact on the operation of the system; a concentration of 1 mL/L was suitable for the normal operation of partial nitrification.

3.3. Isotope tracer method

Table 2 shows the experimental results of the isotope experimental group (IEG). The data were analyzed via the Student *t* test. Compared with the blank sample, the NH_4^+-N conversion, NO_2^--N accumulation, and average carbon sequestration rates of IEG were relatively stable, and there were no significant differences (p-value $>$ 0.05). In terms of isotope detection in sludge, there were no significant differences between the carbon content of the blank sample and IEG (p-value $>$ 0.05). However, the abundance of $\delta^{13}C$ and ^{13}C% content (VPDB) were significantly lower than those of the blank sample (p-value $<$ 0.01). Furthermore, the isotope content in the sludge samples was greater in the IEG after $NaH^{13}CO_3$ labeling than it was in the blank sample. The standard deviation between parallel samples was small, indicating that the test results had good reproducibility. The results further showed that the IC source was effectively metabolized by the microorganisms in partial nitrification sludge, and a carbon fixation pathway gene was present.

3.4. qPCR

The Calvin cycle is a major CO_2 fixation pathway in nearly all ecosystems. Rubisco is regarded as a key functional enzyme in the Calvin cycle and exists in multiple natural forms (such as forms I, II, III, and IV) (Hanson & Tabita, 2001). The *cbbL* gene is commonly used to encode a large subunit of form I Rubisco (Kusian & Bowien, 1997). In this study, *cbbL*R1 was used as the marker gene of the red-type Rubisco form I *cbbL* gene (Selesi et al., 2005; Wahlund & Tabita, 1997). AOB DNA was analyzed via qPCR to explore the carbon sequestration pathway in partial nitrification. DNA extraction and analyses were carried out by thawing the stored sludge of every group at the end of the experiment. The purity of the extracted DNA was good and met the requirements of subsequent experiments. Therefore, qPCR was performed on the samples.

Fig. 5 shows the average abundance of the *cbbL*R1 gene, and the control group consisted of pre-treatment sludge samples. The copy number of *cbbL*R1 before partial nitrification sludge treatment was 7.50×10^8. The average number of gene copies affected by NH_4^+-N, IC, Ca^{2+} and Mg^{2+}, and microbial accelerant were 1.27×10^9, 1.07×10^9, 1.04×10^9, and 1.10×10^9, respectively. The number of *cbbL*R1 gene copies increased after treatment, and increased most under the influence of nitrogen. The variation range of the gene copy number in partial nitrification sludge under the influence of NH_4^+-N was larger than that under the influence of the other three substrates.

The correlations between *cbbL*R1 gene abundance in partial nitrification sludge under different conditions and influent substrates (nitrogen concentration, IC, Ca^{2+} and Mg^{2+}, and microbial accelerant) are shown in Table 3. The response of *cbbL*R1 gene abundance to nitrogen was slightly greater than its response to the other three substrates. Therefore, functional gene *cbbL*R1, which follows the Calvin cycle carbon sequestration pathway, is likely present in the partial nitrification sludge. The response of *cbbL*R1 gene abundance to nitrogen in AOB was greater than that to IC, Ca^{2+} and Mg^{2+}, and microbial accelerant. There was a significant correlation between *cbbL*R1 and NH_4^+-N concentration, IC concentration.

4. Conclusions

The following conclusions could be drawn from batch simulation experiments of partial nitrification reaction: carbon sequestration rate of partial nitrification was positively correlated with influent NH_4^+-N and negatively correlated with IC. In wastewater containing IC, AOB can immobilize IC into microorganisms through the *cbbL* gene in Calvin cycle and become the carbon source needed for their growth. Finally, AOB released a small amount of CO_2 into the air, so that partial nitrification doesn't need additional organic carbon source to provide the energy for microorganism growth. *CbbL* gene was significantly correlated with the changes of influent NH_4^+-N and IC.

Declaration of Competing Interest

The authors declare that they have no known competing financial interests or personal relationships that could have appeared to influence the work reported in this paper.

Acknowledgements

This research was supported by the National Natural Science Foundation of China [grant numbers 51668013, 51638006]; Guangxi Science and Technology Planning Project under Grant No. GuiKe-AD18126018; Special Funding for Guangxi "BaGui Scholar" Construction Projects.

References

Benson, A.A., Calvin, M., 1950. The Path of Carbon in Photosynthesis VII Respiration and Photosynthesis. J. Chem. Edu. 1 (1), 63–68.
Buchanan, B.B., Arnon, D.I., 1990. A reverse KREBS cycle in photosynthesis: consensus at last. Photosynth. Res. 24 (1), 47–53.
Dong, L.I., Liu, L.Q., Di, W.U., Zhang, G.L., Gao, W.N., Zhang, Z., Zhang, J., 2013. The start-up strategy of shortcut nitrification in SBR under low ammonia at room temperature. China Environ. Sci. 33 (2), 215–220.
Guisasola, A., Petzet, S., Baeza, J.A., Carrera, J., Lafuente, J., 2006. Inorganic carbon limitations on nitrification: experimental assessment and modelling. Water Res. 41 (2), 277–286.
Hanson, T.E., Tabita, F.R., 2001. A ribulose-1,5-bisphosphate carboxylase/oxygenase (RubisCO)-like protein from Chlorobium tepidum that is involved with sulfur metabolism and the response to oxidative stress. Proc. Natl Acad. Sci. 98 (8), 4397–4402.
Gijs, J.K., 2008. Anammox bacteria: from discovery to application. Nat. Rev. Microbiol., 6(4), 320-326.
Jetten, M.S.M., Schmid, M., Schmidt, I., Wubben, M., et al., 2002. Improved nitrogen removal by application of new nitrogen-cycle bacteria. Rev. Environ. Sci. Biotechnol. 1 (1), 51–63.
Jin, Y., Wang, D., Zhang, W., 2016a. Effects of substrates on N_2O emissions in an anaerobic ammonium oxidation (anammox) reactor. Springer Plus 5 (1), 741–752.
Jin, Y., Wang, D., Zhang, W., 2015. Treatment of high-strength ammonia containing wastewater using partial nitritation system with biological selector. Global NEST J. 17 (4), 738–743.
Jin, Y., Wang, D., Zhang, W., 2016b. Use of bamboo charcoal reduced the cultivated anammox seed sludge dosage during the start-up period. Desalin. Water Treat. 57 (43), 20248–20253.
Jin, Y., Zhang, W., 2016. NaH2PO4 as pH buffer in an anaerobic ammonium oxidation (anammox) reactor treating high-strength livestock manure digester liquor. Desalin. Water Treat. 57 (56), 27028–27034.
Kartal, B., Kuenen, J.G., Loosdrecht, M.C.M.v. 2010. Sewage Treatment with Anammox. Science, 328(5979), 702-703.
Kusian, B., Bowien, B., 1997. Organization and regulation of cbb CO_2 assimilation genes in autotrophic bacteria. FEMS Microbiol. Rev. 21 (2), 135–155.
Lackner, S., Gilbert, E.M., Vlaeminck, S.E., Joss, A., Horn, H., Loosdrecht, M.C.M.v., 2014. Full-scale partial nitritation/anammox experiences – an application survey. Water Res., 55, 292-303.
Ma, B., Wang, S., Cao, S., Miao, Y., Jia, F., Du, R., Peng, Y., 2016. Biological nitrogen removal from sewage via anammox: Recent advances. Bioresour. Technol. 200, 981–990.
Ma, X., Jin, Y., Zhang, W., 2019. Effects of Ca^{2+} concentration on anaerobic ammonium oxidation reactor microbial community structure. Water 11 (7), 1341.
Macêdo, W.V., Sakamoto, I.K., Azevedo, E.B., Damianovic, M.H.R.Z., 2019. The effect of cations (Na^+, Mg^{2+}, and Ca^{2+}) on the activity and structure of nitrifying and denitrifying bacterial communities. Sci. Total Environ. 679, 279–287.
Meng, H., Yang, Y.C., Lin, J.G., Denecke, M., Gu, J.D., 2017. Occurrence of anammox bacteria in a traditional full-scale wastewater treatment plant and successful inoculation for new establishment. Int. Biodeterior. Biodegrad. 120, 224–231.
Okabe, S., Oshiki, M., Takahashi, Y., Satoh, H., 2011. Development of long-term stable partial nitrification and subsequent anammox process. Bioresour. Technol. 102 (13), 6801–6807.
Ragsdale, S.W., 1991. Enzymology of the Acetyl-CoA pathway of CO_2 fixation. Crit. Rev. Biochem. Mol. Biol. 26 (3–4), 261–300.
Selesi, D., Schmid, M., Hartmann, A., 2005. Diversity of green-like and red-like ribulose-1,5-bisphosphate carboxylase/oxygenase large-subunit genes (*cbbL*) in differently managed agricultural soils. Appl. Environ. Microbiol. 71 (1), 175–184.
Shively, J.M., van Keulen, G., Meijer, W.G., 1998. Something from almost nothing: carbon dioxide fixation in chemoautotrophs. Annu. Rev. Microbiol. 52, 191–230.
Strous, M., Fuerst, J.A., Kramer, E.H.M., Logemann, S., Muyzer, G., van de Pas-Schoonen, K.T., Webb, R., Kuenen, J.G., Jetten, M.S.M., 1999a. Missing lithotroph identified as new planctomycete. Nature 400 (6743), 446–449.
Strous, M., Heijnen, J.J., Kuenen, J.G., Jetten, M.S.M., 1998. The sequencing batch

reactor as a powerful tool for the study of slowly growing anaerobic ammonium-oxidizing microorganisms. Appl. Microbiol. Biotechnol. 50 (5), 589–596.
Strous, M., Kuenen, J.G., Jetten, M.S.M., 1999b. Key Physiology of Anaerobic Ammonium Oxidation. Appl. Environ. Microbiol. 65 (7), 3248–3250.
Sylvia, H., Georg, F., Adelbert, B., Wolfgang, E., 2002. A bicyclic autotrophic CO_2 fixation pathway in Chloroflexus aurantiacus. J. Biol. Chem. 277 (23), 20277–20283.
Wahlund, T.M., Tabita, F.R., 1997. The reductive tricarboxylic acid cycle of carbon dioxide assimilation: initial studies and purification of ATP-citrate lyase from the green sulfur bacterium Chlorobium tepidum. J. Bacteriol. 179 (15), 4859.
Wang, H., Han, J., Zhang, W., 2019. Effects of NH4 + -N and NO2–N on carbon fixation in an anaerobic ammonium oxidation reactor. J. Environ. Manage. 241 (1), 450–457.
Wang, Y.N., Tsang, Y.F., Wang, L., Fu, X., Hu, J., Li, H., Le, Y., 2018. Inhibitory effect of self-generated extracellular dissolved organic carbon on carbon dioxide fixation in sulfur-oxidizing bacteria during a chemoautotrophic cultivation process and its elimination. Bioresour. Technol. 252, 44–51.
Wei, D., Ngo, H.H., Guo, W., Xu, W., Du, B., Wei, Q., 2018. Partial nitrification granular sludge reactor as a pretreatment for anaerobic ammonium oxidation (Anammox): Achievement, performance and microbial community. Bioresour. Technol. 269, 25–31.
Wenjie, Z., Yuanyuan, Z., Liang, L., Xuehong, Z., Yue, J., 2014. Fast start-up of expanded granular sludge bed (EGSB) reactor using stored Anammox sludge. Water Sci. Technol. 69 (7), 1469–1474.
Yamamoto, T., Takaki, K., Koyama, T., Furukawa, K., 2007. Long-term stability of partial nitritation of swine wastewater digester liquor and its subsequent treatment by Anammox. Bioresour. Technol. 99 (14).
Zhang, W., Deng, Y., Wang, D., C.H., Jin, Y., 2016. Treatment of high-strength rare-earth ammonia wastewater with a two-stage anaerobic ammonium oxidation (anammox) process. Global NEST J. 18 (4), 867–874.
Zhang, W., Jin, Y., 2017. Effects of Fe(II) on N_2O emissions from anammox reactors. Desalin. Water Treat. 63, 1–6.
Zhang, W., Wang, D., Jin, Y., 2018. Effects of inorganic carbon on the nitrous oxide emissions and microbial diversity of an anaerobic ammonia oxidation reactor. Bioresour. Technol. 250, 124–130.
Zhang, W., Wang, H., D.R., J., Jin, Y. 2015. Granular activated carbon as nucleus for formation of anammox granules in an expanded granular-sludge-bed reactor. Global NEST J., 17(3), 508-514.